JOURNAL OF NATURAL PRODUCTS

pubs.acs.org/jnp

Article

Antifungal Norditerpene Oidiolactones from the Fungus *Oidiodendron truncatum*, a Potential Biocontrol Agent for White-Nose Syndrome in Bats

Yudi Rusman,[⊥] Michael B. Wilson,[⊥] Jessica M. Williams, Benjamin W. Held, Robert A. Blanchette, Brianna N. Anderson, Christopher R. Lupfer, and Christine E. Salomon*

Cite This: https://dx.doi.org/10.1021/acs.jnatprod.9b00789

Read Online

ACCESS | Metrics & More | Article Recommendations | Supporting Information

ABSTRACT: White-nose syndrome (WNS) is a devastating disease of hibernating bats caused by the fungus *Pseudogymnoascus destructans*. We obtained 383 fungal and bacterial isolates from the Soudan Iron Mine, an important bat hibernaculum in Minnesota, then screened this library for antifungal activity to develop biological control treatments for WNS. An extract from the fungus *Oidiodendron truncatum* was subjected to bioassay-guided fractionation, which led to the isolation of 14 norditerpene and three anthraquinone metabolites. Ten of these compounds were previously described in the literature, and here we present the structures of seven new norditerpene analogues. Additionally, this is the first report of 4-chlorophyscion from a natural source, previously identified as a semisynthetic product. The compounds PR 1388 and LL-Z1271α were the only inhibitors of *P. destructans* (MIC = 7.5 and 15 μg/mL, respectively). Compounds were tested for cytotoxicity against fibroblast cell cultures obtained from *Myotis septentrionalis* (northern long eared bat) and *M. grisescens* (gray bat) using a standard MTT viability assay. The most active antifungal compound, PR 1388, was nontoxic toward cells from both bat species (IC_{50} > 100 μM). We discuss the implications of these results in the context of the challenges and logistics of developing a substrate treatment or prophylactic for WNS.

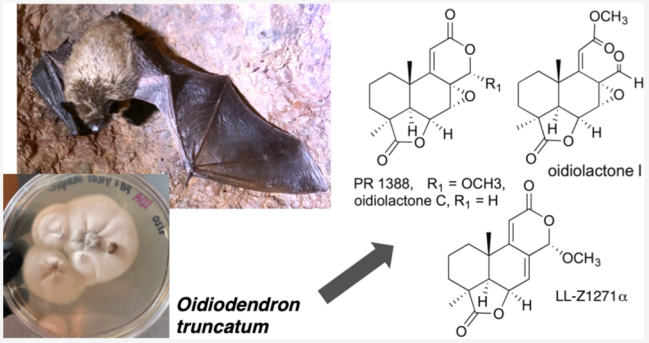

White-nose syndrome (WNS) is an infectious disease of hibernating bats caused by the dermatophytic fungus *Pseudogymnoascus destructans* (formerly *Geomyces destructans*).[1,2] The disease causes high levels of mortality among bat colonies, reaching 95−100% for some highly susceptible species such as *Myotis lucifugus* (little brown bat), *Perimyotis subflavus* (tricolored bat), and *M. septentrionalis* (northern long eared bat). Population declines for *M. septentrionalis* have been so severe that it was listed as threatened under the Endangered Species Act in 2015. In addition to high mortality, WNS is especially concerning due to its rapid spread across North America. Infected bats were first reported from upstate New York in 2006, and WNS has continued to spread across the United States and Canada (Reference USFW maps, https://www.whitenosesyndrome.org/static-page/wns-spread-maps). The disease has been reported in 33 states and seven Canadian provinces (as of August 2019) and recently jumped to Washington state, just nine years after its initial discovery in New York. Evidence suggests that *P. destructans* is an invasive species from Europe or Asia, where it is endemic and does not cause bat mortality.[3,4] The mechanisms of morbidity and mortality are multifactorial, and the disruption of torpor and cascading effects leading to premature emergence from hibernation seem critical to this process.[4,5]

Severe population declines due to WNS are changing bat community structures and species abundance on both temporal and spatial scales.[6,7] The disease also impacts ecosystem services provided by bats, including their critical role in controlling populations of night-flying insects that cause damage to agricultural crops, estimated at $22.9 billion in the U.S. annually.[8] The continued loss of bats due to WNS may result in the use of pesticides to control these insects that would otherwise be eaten by bats, but there are no clear studies that quantify these consequences yet.

There are several WNS treatments in various stages of development. An initial vaccine trial on a small number of bats using orally administered raccoon poxvirus expressing *P. destructans* calnexin and/or serine protease showed promising results with decreased disease symptoms and increased rates of

Received: August 19, 2019

survival.[9] UV light was shown to be highly effective at killing *P. destructans* and is being tested as a method of treatment.[10] Several chemical compounds with *in vitro* fungicidal activity against *P. destructans* have been identified including clinical azole drugs,[11] chitosan,[12] and linoleic acid.[13] Antifungal fumigants may be developed from volatile inhibitors such as 1-octen-3-ol, *trans*-2-hexenal,[14] decanal,[15] and mixtures of volatile compounds produced by rhodococcus bacteria.[16] Deployment of most of these treatments remains a significant challenge because bats inhabit highly inaccessible and dangerous environments (i.e., caves and mines). Regardless of habitat, the resources required to deploy conventional fungicides at the scale required in a way that minimizes ecological disruption may be especially challenging. Since *P. destructans* sheds persistent conidia into the environment,[17] bats treated with antifungals would be at risk for reinfection upon return to hibernacula and therefore require more treatment.

Another promising approach toward a treatment or preventative is to identify living microbes that inhibit the growth of *P. destructans* as a form of biological control.[18] This strategy addresses the aforementioned problems in access and reinfection by providing treatment in the form of an independently transmissible and persistent organism. One previous study demonstrated some success in identifying several strains of *Pseudomonas* isolated from bats with modest antifungal activity.[19] Initial trials with application on bats decreased disease severity when applied at the same time as *P. destructans* conidia, but increased mortality when applied 3 weeks prior to *P. destructans* inoculation,[20] highlighting the challenge of translating laboratory results into *in situ* applications and logistical questions about timing, inoculation, and mechanism.

Our work has focused on isolating bacteria and fungi directly from bats and substrates in their hibernacula and identifying strains with potent activity against *P. destructans*.[21,22] Here, we describe our screening approach with these environmental strains, prioritization rationale, and taxonomic identification of the active isolates. We present the detailed chemical analysis of one of the active fungal species (*Oidiodendron truncatum*) isolated from wood substrate in the Soudan Iron Mine in Tower, Minnesota. Seventeen new and known compounds from two structural classes (norditerpene lactones and anthraquinones) were isolated, identified, and tested for activity against several different pathogenic fungi and mammalian cell lines. These data were used to determine their specificity, structure−activity relationships, and potential cytotoxicity against bat fibroblast cells *in vitro*. This approach should enable a smoother and more reliable and informed transition to field applications for bats. In addition, it facilitates the application of useful organisms and their metabolites to other objectives, such as the development of targeted biopesticides.

RESULTS AND DISCUSSION

Libraries of bacterial and fungal isolates were built from expeditions to the Soudan Iron Mine (near Tower, Minnesota, USA) occurring from 2008 to 2015. This 713.5 m deep underground mine was abandoned in 1962 and now serves as a state park with public tours in the lowest level of the mine. Due to the varying geochemistry throughout the mine, different mine levels have radically different environments that presumably affect the diversity of microbes found there (Figure S1). Gross colony morphology was used to pick bacterial isolates cultured from substrate samples (soil, wood, water, etc.) or bat swabs plated on tryptone soy agar (TSA), International Streptomyces Project 2 agar (ISP2), or marine agar media. Fungal isolates were cultured from substrate samples and swabs plated on malt extract agar (MEA) and selective MEA (containing combinations of streptomycin, benlate, and lactic acid).

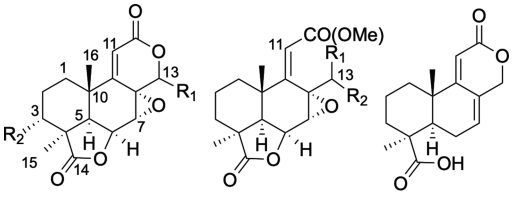

1 R_1 = α-OCH_3, R_2 = H
2 R_1 = β-OH, R_2 = H
3 R_1 = R_2 = H
4 R_1 = α-OH, R_2 = OH
5 R_1 = β-OH, R_2 = OH
6 R_1 = R_2 = OCH_3
7 R_1 = O, R_2 = H
8

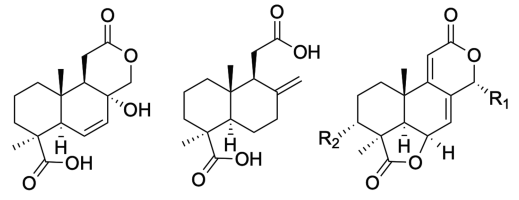

9
10
11 R_1 = OCH_3, R_2 = H
12 R_1 = OCH_3, R_2 = OH
13 R_1 = R_2 = OH

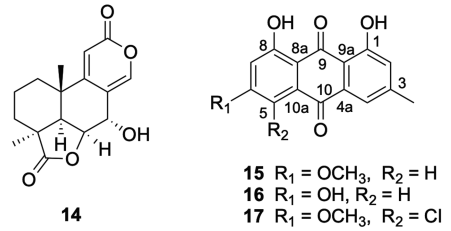

14
15 R_1 = OCH_3, R_2 = H
16 R_1 = OH, R_2 = H
17 R_1 = OCH_3, R_2 = Cl

All 262 bacterial isolates and a phylogenetically representative sample of 121 fungal isolates were screened for anti-*P. destructans* activity via direct competition in overlay or plug assays, respectively. In these assays, 32 fungal and 60 bacterial isolates were active against *P. destructans* (examples of positive results shown in Figure S2). Portions of the 16s rRNA gene and internal transcribed spacer (ITS) sequence of the active bacteria and fungi, respectively, were sequenced for taxonomic analysis. Fermentations of inhibitory isolates were scaled up with solid or liquid media and subsequently extracted using organic solvents. The crude extracts were semipurified using a modified Kupchan solvent partition method,[23] and these fractions were tested against *P. destructans* using a broth dilution assay. A summary of active strains, activity data, and closest taxonomic matches are shown in the Supporting Information (Figure S3).

One of the most inhibitory fungal samples was *O. truncatum* isolated from wood on level 25 of the mine, which displayed contact-dependent inhibition against *P. destructans* in direct competition assays. The crude methanol extract of a 30-day solid rice culture had an MIC_{98} of 62.5 μg/mL in broth dilution assays. The extract was analyzed by reversed-phase HPLC and contained two different suites of closely related compounds (norditerpene lactones **1**−**14** and anthraquinones **15**−**17**). Several metabolites (**1**−**3**, **8**−**11**, **15**, **16**) were known compounds with structures that have been well characterized in the literature, and the new analogues (**4**−**7**, **12**−**14**) were identified in part by comparison of NMR spectroscopic and

https://dx.doi.org/10.1021/acs.jnatprod.9b00789
J. Nat. Prod. XXXX, XXX, XXX−XXX

mass spectrometric data to published information. Anthraquinone **17** was previously reported as a semisynthetic compound, but this is the first report as a natural product.

Compounds **1**−**3** were isolated as the major compounds and identified as the previously reported norditerpene PR 1388 (**1**, 65.2 mg) and oidiolactones D (**2**, 50.4 mg) and C (**3**, 12.3 mg) by comparison of their NMR, MS, and optical rotation data to reported values.[24−26]

Oidiolactone G (**4**, 3.2 mg) was isolated as a white solid with the molecular formula $C_{16}H_{18}O_7$ determined by HRAPCI-MS. Three singlet methines at δ_H 4.00 (H-7), 5.40 (H-13), and 6.04 (H-11), two doublet methines at δ_H 2.06 (H-5) and 4.94 (H-6), two methylenes between δ_H 1.96 and 1.67 (H_2-1 and H_2-2), and two singlet methyls at δ_H 1.33 (H_3-15) and 1.17 (H_3-16) in the NMR spectrum suggested a close structural relationship to compound **2** (Table 1).[24,25] However, an extra signal at δ_H 4.39 was present for **4**, and the formula indicated an additional oxygen. A correlation of H-3 to an oxygen-bonded carbon at δ_C 66.4 in the HMQC spectrum and HMBC correlations between this carbon and H_3-15, H-5, H-1a/b, and H-2a/b established the presence of a hydroxy group at C-3. The coupling constants for H-3 (dd, J = 9.8, 3.5) indicated an axial orientation. Additionally, the configuration at C-3 was supported by an upfield shift (δ_C 16.5) of the C-15 methyl (compared to **2**, δ_C 24.1) due to interaction with the equatorial OH at C-3. The NOESY spectrum showed correlations of H_3-16 to H-3, H-7, and H-13, indicating that these protons were on the same face of the molecule and establishing the relative configuration of C-13 (Figure 1). The mutual NOESY correlations between H-5, H-6, and H_3-15 established their positions on the opposite face.

Table 1. ^{1}H and ^{13}C Data for 4 and 5 (δ in ppm, J in Hz) in $CDCl_3$

	4		5	
position	δ_C	δ_H (J in Hz)	δ_C	δ_H (J in Hz)
1a	28.0	1.91 m	27.8	1.88 m
b		1.71 m		1.72 m
2a	26.5	1.96 m	27.0	1.96 m
b		1.67 m		1.67 m
3	66.4	4.39 dd (9.8, 3.5)	66.4	4.41 dd (10.3, 4.0)
4	47.5		47.4	
5	44.0	2.06 d (4.7)	44.0	2.01 d (4.7)
6	72.8	4.94 d (4.7)	72.6	4.94 d (4.7)
7	53.2	4.00 s	53.9	3.91 s
8	56.3		56.2	
9	157.1		155.2	
10	35.4		34.9	
11	119.0	6.04 s	117.4	5.98 s
12	162.1		161.6	
13	99.5	5.40 s	103.8	4.79 s
14	180.5		180.3	
15	16.5	1.33 s	16.1	1.32 s
16	28.0	1.17 s	26.6	1.13 s

Epi-oidiolactone G (**5**, 2.3 mg) was isolated as a stereoisomer of **4**, with a nearly identical retention time during HPLC purification. The ^{1}H and ^{13}C NMR data and 2D NMR correlations were very similar (Table 1), although carbon signals C-9−C-12 were upfield compared to the analogous signals for **4**. The NOE correlation between H-13 and H_3-16 disappeared, and the proton signal for H-13 was shifted upfield by 0.61 ppm, suggesting an inversion of the C-13 stereocenter.

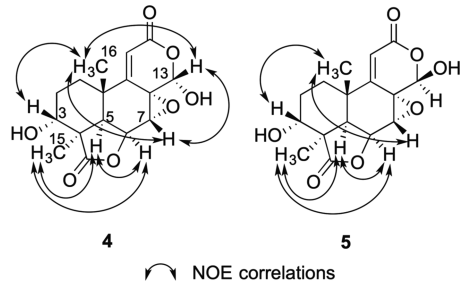

Figure 1. NOE correlations of compounds **4** and **5**.

All other NOE correlations matched the data for compound **4**, indicating the same relative configuration for all other centers. These observations were supported by an optical rotation value of $[\alpha]^{23}_D$ −5.7 (c 0.035, CH_2Cl_2) for **5**, compared to $[\alpha]^{23}_D$ +33 (c 0.115, CH_2Cl_2) for compound **4**.

The molecular formula of oidiolactone H (**6**, 1.4 mg) was determined as $C_{19}H_{26}O_7$ by HRAPCI-MS, with one less double-bond equivalent compared to **1**−**5**. Analysis of the ^{1}H and ^{13}C NMR data (Table 2) revealed the presence of three methoxy groups in the molecule. The HMBC correlations of the C-12 carbonyl to a singlet methine at δ_H 5.84 (H-11) and methoxy protons at δ_H 3.76 (OCH_3-12) established the position of one methoxy at C-12, indicating an opening of the δ-lactone system. The geminal position of the other two methoxys was assigned by HMBC correlations of δ_H 3.54 and 3.34 to a single carbon signal at δ_C 103.5 (C-13), as well as the correlations of H-13 to δ_C 58.4 (OCH_3-13a) and δ_C 57.4 (OCH_3-13b). The position of this dimethoxy side chain at C-8 was established by HMBC correlations of H-13 (δ_H 4.97) to C-7 (δ_C 51.4). The relative configurations of C-4, C-5, and C-6 were determined by the mutual NOE correlations between H-5, H-6, and H_3-15 (Figure

Table 2. ^{1}H and ^{13}C Data for 6 and 7 (δ in ppm, J in Hz)

	6[a]		7[b]	
position	δ_C	δ_H (J in Hz)	δ_C	δ_H (J in Hz)
1a	31.9	1.51 m	30.6	1.58 m
b		1.33 m		1.42 m
2a	18.1	1.65 m	18.1	1.55 m
b		1.65 m		1.50 m
3a	28.6	2.25 m	28.6	2.01 m
b		1.27 m		1.36 m
4	41.9		41.8	
5	49.5	1.56 d (4.4)	46.8	1.72 d (4.0)
6	72.5	4.83 d (4.4)	71.7	5.13 d (4.0)
7	51.4	3.92 s	54.4	4.19 s
8	61.1		62.1	
9	158.6		155.5	
10	39.8		37.7	
11	118.0	5.84 s	118.5	5.95 s
12	166.2		165.8	
13	103.5	4.97 s	195.6	9.02 s
14	180.1		179.8	
15	25.5	1.17 s	24.8	1.16 s
16	19.4	1.05 s	19.3	0.85 s
OMe-12	51.7	3.76 s	52.1	3.63 s
OMe-13	58.4	a. 3.54 s		
	57.4	b. 3.34 s		

[a]In $CDCl_3$. [b]In DMSO-d_6.

https://dx.doi.org/10.1021/acs.jnatprod.9b00789
J. Nat. Prod. XXXX, XXX, XXX−XXX

2). The spatial orientation of the epoxide at C-7 was established by the NOE correlation of H-7 to H_3-16.

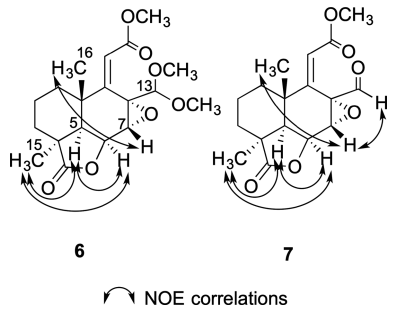

Figure 2. NOE correlations of compounds **6** and **7**.

Oidiolactone I (**7**, 5.7 mg) was isolated as a white solid with a molecular formula of $C_{17}H_{20}O_6$. Comparison of the NMR data suggested a structural relationship to **6** (Table 2). The major differences in the ^{1}H spectrum were the loss of the two geminal methoxy signals and addition of a downfield aldehyde signal at δ_H 9.02. Analysis of the HMBC data revealed a direct correlation between δ_H 9.02 (H-13) and a carbonyl at δ_C 195.6 (C-13) and a three-bond correlation to an oxygenated carbon δ_C 62.1 (C-8), indicating the presence of an aldehyde at C-8. The orientation of the epoxide was determined by an NOE correlation between H-7 and H_3-16 (Figure 2). The remaining HMBC, COSY, and NOE correlations of this compound were similar to those of **6**.

Compound **7** is also the C-12 methoxy derivative of the open-chain form of oidiolactone D (**2**) previously hypothesized to be in equilibrium with the hemiacetal structure.[25]

The remaining norditerpene lactones isolated (**8**−**14**) lacked the C-7/C-8 epoxide. The known compounds oidiodendronic acid[24] (**8**, 8.1 mg), oidiolactone E[25] (**9**, 1.3 mg), LL-Z1271β[27] (**10**, 3.9 mg), and LL-Z1271α[28] (**11**, 50.8 mg) were identified by comparison of the NMR, mass, and optical rotation data with literature values.

Oidiolactone J (**12**, 5.2 mg) was isolated as a white solid with a molecular formula of $C_{17}H_{20}O_6$ based on HRESIMS analysis. Comparison of the NMR and mass data suggested a close structural relationship to LL-Z1271 α (**11**), with one additional oxygen (Table 3). The position of a hydroxy group at C-3 was established by the observation of HMBC correlations of H-3 (δ_H 4.18) to C-1, C-14, and C-15 as well as correlations of H-2, OH-3, and H_3-15 to C-3 (δ_C 64.2). Both H-3 and H-13 displayed NOE correlations to CH_3-16, indicating their position on the same face of the molecule (Figure 3). The remaining HMBC, COSY, and NOE correlations of this compound were similar to those of compound **11**.

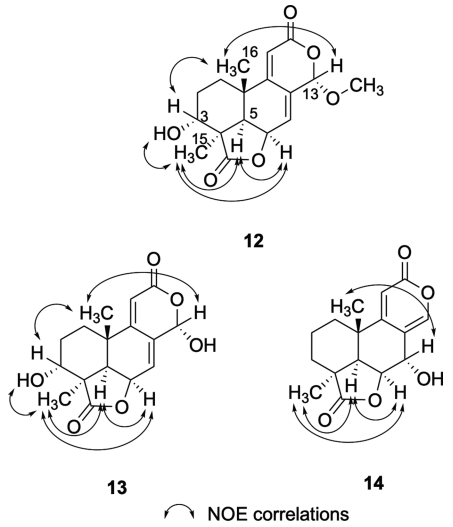

Figure 3. NOE correlations of compounds **12**−**14**.

Table 3. ^{1}H and ^{13}C Data for 12−14 (δ in ppm, J in Hz) in DMSO-d_6

	12		13			14	
position	δ_C	δ_H (J in Hz)	δ_C	δ_H (J in Hz)	position	δ_C	δ_H (J in Hz)
1a	28.3	1.86 m	28.0	1.83 m	1a	32.2	1.85 m,
b		1.68 m		1.68 m	b		1.47 m
2a	27.0	1.77 m	26.9	1.77 m	2a	17.5	1.75 m
b		1.62 m		1.63 m	b		1.69 m
3	64.2	4.18 m	64.2	4.19 m	3a	28.4	2.27 m
					b		1.43 m
4	47.6		47.6		4	42.0	
5	46.8	2.17 d (5.0)	47.2	2.16 d (5.0)	5	50.1	1.80 d (5.8)
6	71.2	5.21 dd (5.0, 4.3)	71.2	5.19 dd (5.0, 3.9)	6	84.0	4.78 dd (5.8, 4.0)
7	123.7	6.44 d (4.3)	124.0	6.46 d (3.9)	7	68.0	5.16 dd (4.0, 1.5)
8	132.0		133.5		8	115.5	
9	157.4		156.1		9	163.6	
10	33.9		33.6		10	36.4	
11	111.5	5.77 s	110.5	5.72 s	11	106.9	6.02 s
12	162.3		162.9		12	162.5	
13	100.9	6.00 s	94.9	6.01 br	13	149.8	7.70 d (1.5)
14	180.6		180.6		14	180.6	
15	16.0	1.23 s	15.9	1.23 s	15	25.7	1.29 s
16	26.3	1.05 s	25.7	1.03 s	16	22.2	1.06 s
OMe-13	56.7	3.59 s					
OH-3		4.96 d (5.2)		4.95 d (5.3)			

https://dx.doi.org/10.1021/acs.jnatprod.9b00789
J. Nat. Prod. XXXX, XXX, XXX−XXX

Oidiolactone K (**13**, 6.7 mg) was obtained as a white powder with the molecular formula $C_{16}H_{18}O_6$. Comparison of the NMR data suggested that the structure was closely related to **12** (Table 3), but the mass analysis indicated the loss of one methyl group (−15 amu). Additionally, the C-13 O-methyl group signal was absent in the ^{1}H spectrum and the compound was more polar, as indicated by reduced solubility in $CDCl_3$ and reduced retention time during HPLC purification. These observations indicated the presence of a hydroxy group at C-13. The relative configuration of C-13 was determined by an NOE correlation of H-13 to H_3-16. The remaining HMBC, COSY, and NOE correlations of this compound were similar to those observed in compound **12**.

Oidiolactone L (**14**, 2.5 mg) was isolated as colorless crystals with a molecular formula of $C_{16}H_{18}O_5$ deduced from the HRAPCIMS data. This compound differs from the previous structures by the presence of a C-8/C-13 double bond, indicated by a doublet at δ_H 7.70 (H-13) with allylic coupling to H-7 (J = 1.5 Hz) and HMBC correlations to C-8 and C-9. A hydroxy group at C-7 was indicated by an HMQC correlation of H-7 to a carbon at δ_C 68.0 (C-7) and supported by HMBC correlations of H-6, H-11, and H-13 to C-7. The relative configuration of C-7 was determined by observation of an NOE correlation between H-7 and CH_3-16. The NOE correlations of H-6 with CH_3-15 and H-5 indicate their position on the opposite face of the molecule, consistent with the analogous substructures of **1**−**7** and **11**−**13**. The ^{1}H and ^{13}C NMR data for compound **14** are shown in Table 3.

The absolute configurations of norditerpene lactones **5**, **7**, and **12** were determined by circular dichroism spectroscopy and comparison to previously reported compounds. The CD spectra of compounds **1**, **5**, **7**, **11**, and **12** all showed a negative Cotton effect at 265−270 nm, indicating that the configuration of the common chiral centers was 4*S*, 5*R*, 6*S*, 10*S*.[24,29] We also assume the same core configuration for the biosynthetically related remaining compounds in this series (**4**, **6**, **13**, and **14**), thus defining the absolute configurations for all new compounds as depicted.

In addition to norditerpenes, three anthraquinone metabolites were also isolated. Compounds **15** (5.4 mg) and **16** (2.2 mg) were identified as physcion (parietin) and emodin, respectively.[30] Compound **17** (2.4 mg) was isolated as orange crystals with the molecular formula $C_{16}H_{11}ClO_5$ derived from analysis of the HRESIMS data. The presence of only three aromatic singlets and a mass difference due to chlorine distinguished compound **17** from **15**. The position of the methoxy group at C-6 was supported by HMBC correlations of the O-CH_3 protons and H-7 to an oxygenated aromatic carbon at δ_C 160.8. The C-5 chlorine substitution was corroborated by HMBC correlations of H-7 to a nonprotonated carbon at δ_C 112.6 (C-5). Compound **17** has been previously reported as a semisynthetic compound (4-chlorophyscion[31] and 5-chloroparietin[32]) in studies of chlorination of lichen anthraquinones, but, to our knowledge, this is the first report of its isolation from nature. Due to the lack of complete NMR data in the literature for this compound, the full data set is provided in the Supporting Information (Figures S53−S56).

All compounds were tested against a panel of human bacterial and fungal pathogens as well as the bat fungal pathogen *P. destructans* to determine their potency, specificity, and structure−activity relationships. None of the compounds inhibited bacterial growth, but three compounds (**1**, **3**, and **11**) exhibited antifungal activity against *Cryptococcus neoformans* and *Candida albicans*, and compound **7** was active against *C. neoformans* (MIC ≤ 30 μg/mL, Table 5). Compounds **1** and **11** also inhibited the growth of *P. destructans* with MIC values of 7.5 and 15 μg/mL, respectively. Analysis of structure−activity relationships indicates that the presence of a hydroxy moiety at C-13 in the epoxide dilactone series abolishes the antifungal activity (i.e., **2**, **4**, **5**). For the 7,9(11)-diene 12,13-olide series, the hydroxy at C-3 leads to a loss of activity (**12**), and inactive compound **13** has both the C-13 and C-3 hydroxy groups. Although the mechanism of action is not yet known for this class of antifungal compounds, one earlier study identified LL-Z1271α (**11**) as an inhibitor of protein synthesis in *Saccharomyces cerevisiae*.[33]

Table 5. Antifungal and Cytotoxicity Activity of Compounds 1−17[a]

	fungal growth inhibition, MIC, μg/mL			cytotoxicity, IC_{50}, μM		
	P. destr.	*C.alb.*	*C. neo.*	*M. gris.*	*M. sept.*	*H. sap.*
1	7.5	20	17.5	102.7	75.6	>100
2	>30	>100	>100	>100	>100	>100
3	>30	20	12.5	85.4	89.7	40.7
4	>30	>100	>100	72.4	83.7	>100
5	nt	>100	>100	>100	>100	>100
6	>30	>100	>100	>100	>100	nt
7	>30	50	30	5	12.5	34.3
8	>30	>100	>100	70	>100	80 1
9	nt	>100	>100	>100	>100	nt
10	>30	>100	>100	>100	>100	>100
11	15	12.5	10	19.6	20.2	21.4
12	>30	>100	>100	>100	>100	>100
13	>30	nt	nt	>100	>100	>100
14	>30	>100	>100	>100	>100	>100
15	>30	>100	>100	nt	nt	>100
16	>30	>100	>100	nt	nt	>100
17	>30	55	45	nt	nt	>100

[a]*P destr.* = *Pseudogymnoascus destructans*, *C. alb.* = *Candida albicans*, *C. neo.* = *Cryptococcus neoformans*, *M. gris.*= *Myotis grisescens*, *M. sept.* = *Myotis septentrionalis*, *H. sap.* = *Homo sapiens* HaCAT fibroblast cell line.

In order to further characterize the producing fungus as a potential biological control agent for application on or near live bats, we tested a subset of the isolated compounds for cytotoxicity against bat skin cells. *In vitro* cytotoxicity of topical compounds tested with cultured fibroblast cells has been previously correlated to irritation of intact skin in human volunteers.[34] Primary fibroblast cell cultures were established from a WNS-susceptible species (*Myotis septentrionalis*, northern long eared bat) and a resistant species (*M. grisescens*, gray bat). Compounds were tested against both cell lines using a standard MTT cell viability assay over 72 h, and the results are reported in Table 5. Compounds were also tested against a human primary dermal fibroblast cell line for comparison.

The most potent inhibitor of *P. destructans* (**1**) was not cytotoxic toward cell cultures of either bat species. Compound **11** was 2-fold less active toward *P. destructans*, but exhibited weak cytotoxicity toward fibroblast cells of both bat species (IC_{50} ~20 μM). Oidiolactone I (**7**) was the only compound with no *P. destructans*activity and some bat cell cytotoxicity (IC_{50}: 5 μM, *M. grisescens* and 12.5 μM, *M. septentrionalis*). All other

https://dx.doi.org/10.1021/acs.jnatprod.9b00789
J. Nat. Prod. XXXX, XXX, XXX−XXX

compounds tested were nontoxic toward bat fibroblast cells (IC_{50} > 80 μM).

Comparison of cytotoxicity activity with fibroblast cells from WNS-resistant and -susceptible bat species demonstrated that there was little difference between them for this compound series. We also included a cell viability assay with primary human fibroblast cells (HaCAT) and found that there were some differences in IC_{50} values compared to bat fibroblast cytotoxicity. Oidiolactone C (**3**) was twice as toxic toward human fibroblasts, and oidiolactone H (**7**) was 7-fold less active against the human cells. These results suggest that *in vitro* testing of topical compounds or extracts with human fibroblast cell lines is not necessarily indicative of cytotoxicity for relevant bat species. We do not yet know how to translate *in vitro* cell-based toxicity data to potential irritation or toxicity toward intact bat skin, especially in the context of substrate application of biocontrol strains that might not come into contact with hibernating bats at significant levels.

This current study represents a detailed chemical analysis of only one of 92 leads generated by our isolation and screening strategy. Due to the unique geochemical environments within the Soudan mine, and previous and ongoing chemical studies on subterranean microbes, we expect to find diverse chemistry and antifungal activities within this set of organisms.[22,23] Compound isolation and structure elucidation allow us to better understand biological control candidates by providing specific information about structure−activity relationships, potency of individual compounds, and potential toxicity. Biological control may be a good strategy for the mitigation of WNS because it theoretically overcomes many of the logistical challenges associated with potential treatments. The application of live microbes that are already adapted to cave and mine surfaces may address the issues of scope, scale, and inaccessibility of hibernacula through self-perpetuation and self-spreading. Biological control on hibernaculum substrates could be used to create and maintain an inhospitable environment for *P. destructans* and restore a balance disrupted by this invasive species. One of the risks of this approach is potentially disrupting other hibernacula-associated microbial communities and macro-fauna. We hope to mitigate this risk by selecting candidate organisms from the original hibernaculum environment. However, there are also critical logistical challenges associated with the implementation of biocontrol, including dosage, timing, and frequency of application and the high level of inhibition necessary for disease suppression.[20,35]

Oidiodendron spp. have a worldwide distribution and are commonly isolated from soil, decaying plant material, and subterranean environments.[36−39] Several species have also shown ericoid mycorrhizal relationships and are associated with the roots of *Betula*, *Picea*, and *Abies* trees in boreal forests.[40,41] Although only *O. truncatum* was fully evaluated in this study, thirty-five isolates of six different *Oidiodendron* species (*Myxotrichum arcticum*; an anamorph of *Oidiodendron*, *O. echinulatum*, *O. griseum*, *O. nigrum*, *O. tenuissimum*, and *O. truncatum*) were obtained from eight levels of the Soudan mine (Figure S4). Cultures were mainly isolated from wood; however, several isolates were obtained from swabs of the mine wall and one isolate was obtained from a dead bat. Preliminary plug assays with six of these isolates against *P. destructans* showed that two other *O. truncatum* strains from different mine levels were also inhibitory (Figure S4). This wealth of untapped potential makes *Oidiodendron* spp. a good lead for biological control. Considering that most isolates came from substrate samples, the best application of *Oidiodendron* spp. is probably as a substrate-level suppressor of *P. destructans* in the environment, rather than as a treatment applied directly to bats. The value of this role cannot be understated, as *P. destructans* conidia are persistent in bat hibernacula[35] and their suppression may be key to the long-term control of white-nose syndrome in bat populations. The next logical steps are *in vitro* and *in situ* substrate growth suppression, *in vivo* bat toxicity or irritation, and disease suppression trials. Additional testing will be needed to measure the quantity of each compound produced in natural settings and to determine if *O. truncatum* can grow, expand, and inhibit *P. destructans* on various natural substrates to reduce the spread or development of WNS in bats.

EXPERIMENTAL SECTION

General Experimental Procedures. Reagents were purchased from Fisher Scientific unless otherwise noted. Optical rotations were measured on a Rudolph Research Analytical Autopol III polarimeter. IR spectra were obtained using a JASCO 4100 FT-IR spectrophotometer. Low- and high-resolution mass analyses were performed using an Agilent TOF II mass spectrometer with a dual ESI and APCI source. A JASCO 200 system was used to record the CD spectra. Standard 1D and 2D NMR spectra were recorded on a Varian 600 MHz and Bruker 400 MHz. Proton and carbon chemical shifts are reported in ppm and referenced with the ^{1}H and ^{13}C signals of solvents. Flash chromatography separations were performed using a Teledyne ISCO Combiflash Rf system. TLC separations were performed using Whatman silica gel 60 F_{254} aluminum backed TLC plates. HPLC separations were performed with an Agilent 1200 instrument with a PDA detector system. CD spectra were obtained with a Jasco J-815 CD spectrometer.

Microorganisms and Culture Conditions. Bacteria were isolated from bat swabs or substrate samples collected during annual sampling trips to the Soudan Iron Mine State Park, Tower, Minnesota, between 2008 and 2015. Bats and solid substrate surfaces were swabbed with sterile, phosphate-buffered saline (PBS)-wetted sampling swabs (1 mL of PBS added to Puritan Hydraflock swabs, 25-3306-H BT), while loose substrates including small wood segments and rock/sediments were collected into sterile whirl packs. All samples were kept cool and transported to the laboratory. General isolation and sequencing methods for fungi: Substrate samples were aseptically cut into smaller segments and cultured for fungi using several types of growth media: 1.5% Difco MEA, MEA with 0.1 g of streptomycin sulfate added after autoclaving, and a semiselective media for Basidiomycetes that included MEA with 2 g of yeast, 0.06 g of Benlate, 0.1 g of streptomycin sulfate, and 2 mL of 85% lactic acid added after autoclaving. Swabs of substrates and bats were also directly streaked across the various types of media. Plates were incubated at 20 °C. Following incubation, fungi that grew from substrate materials were transferred to another plate to obtain pure cultures. Genomic DNA was extracted using a cetyltrimethylammonium bromide extraction protocol, and the ITS regions of rDNA were amplified by PCR using the ITS1F/ITS4 primer pair following the methods of Blanchette et al., 2016.[41] Sanger sequencing was carried out with both forward and reverse primers using an ABI 3730xl DNA sequencer (Applied Biosystems, Foster City, CA, USA). A consensus sequence was assembled from both reads using Geneious 7.1.[42] The BLASTn algorithm was used to compare sequences to those in GenBank to determine the best possible match to known isolates. One isolate from each fungal species, based on ITS similarity to described species in GenBank, was randomly chosen for anti-*P. destructans* activity screening. The isolate *O. truncatum* (MN0802960) was identified by its close match (99% ITS identity) to a type specimen in GenBank in addition to phenotypical analysis. Once this strain was identified as being highly active, five additional isolates of *Oidiodendron* spp. were also tested in plug assays: *O. nigrum* MN080297, *O. truncatum* MN080293 and MN080294, and *O. tenuissimum* MN080298 and MN080295.

https://dx.doi.org/10.1021/acs.jnatprod.9b00789
J. Nat. Prod. XXXX, XXX, XXX−XXX

General Isolation and Sequencing Methods for Bacteria. Subsamples of solid substrates were partitioned into 1 mL of PBS in a 2 mL microcentrifuge tube and vortexed for 10 s, while swabs were similarly vortexed in their sample tubes. A 250 μL aliquot of each sample was heat shocked in a 55 °C water bath for 15 min to select for spore-forming bacteria. Aliquots of each sample (50 μL) were spread onto separate 1.5% agar plates of TSA (Difco BD 236950), ISP2 (BD 277010), and SCA (10 g starch, 2 g KNO_3, 2 g K_2HPO_4, 2 g NaCl, 0.3 g casein, 0.05 g $MgSO_4{\cdot}7H_2O$, 0.02 g $CaCO_3$, 0.01 g $FeSO_4{\cdot}7H_2O$) enriched with 0.25 μg/mL nystatin and 0.5 μg/mL cyclohexamide to suppress fungal growth. Morphologically distinct colonies were picked and streaked out onto new plates as they became apparent. If samples were too concentrated for individual colonies to be apparent, then serial dilutions were plated using the same method. Passages continued until only one bacterial morphotype was present on a plate, then morphologically characterized, and preserved by adding sterile glycerol (25% final concentration) to an overnight liquid culture and freezing at −80 °C in 2 mL screw top tubes. 16S rRNA gene sequencing was used to determine the identity of active bacteria isolates. Liquid seed cultures (10 mL) of isolates showing activity in the overlay assays (see below) were pelleted by centrifugation and stored at −80 °C. DNA was extracted from pellets using the MoBio UltraClean DNA isolation kit (12224-250) according to manufacturer specifications and stored at −20 °C. The 16S rRNA gene was amplified from genomic templates using 27F and 1492R 16s rRNA universal bacterial primers[43] with GoTaq Green master mix (M7123). Sanger sequencing was carried out with both forward and reverse primers using an ABI 3730xl DNA sequencer (Applied Biosystems).

Antifungal Screening Assays. Overlay assays were used to screen bacterial isolates for anti-*P. destructans* activity. Seed cultures were made by inoculating TS, ISP2, or SC liquid media (5 mL) and incubating at 25 °C for 3−7 days until visibly opaque. Each seed culture (2 μL) was spotted onto 1.5% TSA, ISP2, or SCA solid agar in 10 × 150 mm plates, with 2−4 different cultures spotted per plate. Plates were incubated until spots grew into single colonies ∼10−15 mm in diameter, 3−7 days. Plates were then overlaid with molten 1% Sabouraud dextrose agar (SDA) (cooled to ∼50 °C) and then spread inoculated with 2500 *P. destructans* conidia in 100 μL of sterile water. Overlaid plates were incubated at 15 °C for 14 days, at which time a visible lawn of *P. destructans* had grown across the plate surface. Bacterial colonies that produced zones of growth inhibition > 1 mm (radius from edge of antagonist colony) were considered active.

Plug competition assays were used to screen a genetically representative subset of fungal isolates. *P. destructans* and Soudan Mine (SM) fungal isolates were grown on SDA plates as above. Plugs of 5 mm^3 were cut from the outside edge of growing colonies and placed colony-side down 3 cm apart on a new SDA plate. Age-paired control plates without competing SM isolates were similarly created. Fungal isolates were considered active if the diameter of the resulting *P. destructans* colony was visibly less than the control. Sometimes inhibition was clearly due to chemical diffusion, but other times it required contact between the *P. destructans* and SM isolate colonies.

Extraction, Isolation, and Identification of Compounds from *Oidiodendron truncatum*. A seed culture of the fungus was grown on a potato dextrose agar plate for 10 days at room temperature. Approximately one-eighth of the agar plate was chopped into small pieces and vortexed in a 50 mL conical tube with 5 mL of PBS buffer. This agar suspension was then used to inoculate rice medium (3 × 1 L flasks containing 100 g rice and 100 mL of water), which was cultured at room temperature for 30 days.

The rice cultures were exhaustively extracted with EtOAc and MeOH (3 × 300 mL for each solvent). Extracts were combined, concentrated, and successively partitioned with 300 mL of EtOAc, *n*-hexane, and *n*-BuOH. The EtOAc fraction (1668 mg) was purified by flash chromatography (Teledyne ISCO Combiflash Rf; solid-phase Redisep Rf 24 g silica; gradient elution 0−100% of EtOAc/*n*-hexane for 35 min; flow rate 25 mL/min). Fractions were pooled into 18 fractions (F1−F18) based on TLC analysis. Fraction F4 (88.6 mg) was further separated using semipreparative HPLC (gradient elution 35−100% acetonitrile/H_2O for 22 min; flow rate 3 mL/min, column: Vision HT-C_{18} 10 × 250 mm) to generate **7** (5.7 mg), **15** (5.4 mg), and **16** (2.2 mg). Subfraction F4.5 (4.5 mg) was repurified using two subsequent analytical-scale HPLC separations (gradient elution 40−80% acetonitrile/H_2O for 17 min; flow rate 1 mL/min, column: Lux cellulose-4, 4.6 × 250 mm) to give **6** (1.4 mg). Subfraction F5 (5.4 mg) was repurified using analytical-scale HPLC (gradient elution 60−80% acetonitrile/H_2O for 11 min; flow rate 1 mL/min, column: Lux cellulose-4, 4.6 × 250 mm) to isolate **17** (2.4 mg). Subfraction F7 (851.8 mg) was separated by flash chromatography (Teledyne ISCO Combiflash Rf; solid-phase Redisep Rf 50 g C_{18}; step gradient elutions: 30−50% of MeOH/H_2O for 17 min, followed by 50−80% of MeOH/H_2O for 5 min and 80−100% of MeOH/H_2O for 2 min; flow rate 40 mL/min) to give **2** (50.4 mg), **3** (12.3 mg), **11** (50.8 mg), and **8** (8.1 mg). Subfraction F10 (260.4 mg) was separated by semipreparative HPLC (gradient elution 25−60% acetonitrile/H_2O for 20 min; flow rate 3 mL/min, column: Vision HT-C_{18} 10 × 250 mm) to obtain **1** (65.2 mg), **14** (2.5 mg), and **10** (3.9 mg). Subfraction F10.7 was repurified by analytical-scale HPLC separation (gradient elution 20−40% acetonitrile/H_2O for 12 min; flow rate 1 mL/min, column: ODS hypersil 4 × 250 mm) to isolate **9** (28.5 mg). Subfraction F10.11 was purified using analytical-scale HPLC (gradient elution 35−57.5% acetonitrile/H_2O for 11 min; flow rate 1 mL/min, column: Altima HP C_{18}, 4.6 × 250 mm), which yielded **9** (1.3 mg). Subfraction F11 (26.4 mg) was subjected to three consecutive semipreparative HPLC separations (gradient elution 25−60% of acetonitrile/H_2O for 20 min for each step; flow rate 3 mL/min, column: Vision HT-C_{18} 10 × 250 mm), which yielded **4** (3.2 mg) and **5** (2.3 mg). Subfraction F15 (19.2 mg) was purified using semipreparative HPLC (gradient elution 15−60% acetonitrile/H_2O for 23 min; flow rate 3 mL/min, column: Vision HT C_{18}, 4.6 × 250 mm) to give compound **12** (6.7 mg). Further separation of F15.4 using analytical-scale HPLC separation (gradient elution 25−30% acetonitrile/H_2O for 7 min; flow rate 1 mL/min, column: Lux cellulose-4, 4.6 × 250 mm) produced compound **13** (5.2 mg).

*Oidiolactone G (**4**):* white solid; $[\alpha]^{23}_D$ +33 (*c* 0.115, CH_2Cl_2); UV (CH_2Cl_2) λ_{max} (log ε) 205 (2.69), 230 (2.77), 245 (2.77); IR (film) ν_{max} 3738, 3020, 2975, 2905, 2357, 2350, 2320, 1774, 1717, 1508, 1456, 1275, 1260, 1199, 1103, 1028, 957 cm^{-1}; ^1H NMR (600 MHz) and ^{13}C NMR (151 MHz), see Table 1; HRAPCI-MS *m*/*z* 321.0992 $[M - H]^-$ (calcd for $C_{16}H_{17}O_7$, 321.0974).

*Epi-oidiolactone G (**5**):* white solid; $[\alpha]^{23}_D$ −5.7 (*c* 0.035, CH_2Cl_2); UV (CH_2Cl_2) λ_{max} (log ε) 205 (2.89), 230 (2.96), 245 (2.97) ; IR (film) ν_{max} 3727, 3020, 2928, 2357, 2340, 1775, 1732, 1456, 1375, 1275, 1260, 1197, 1144, 1103, 1035, 984, 954 cm^{-1}; ^1H NMR (600 MHz) and ^{13}C NMR (151 MHz), see Table 1; HRAPCI-MS *m*/*z* 321.0994 $[M - H]^-$ (calcd for $C_{16}H_{17}O_7$, 321.0974).

*Oidiolactone H (**6**):* white solid; $[\alpha]^{23}_D$ +24 (*c* 0.065, CH_2Cl_2); UV (CH_2Cl_2) λ_{max} (log ε) 205 (2.86), 230 (2.92), 245 (2.93); IR (film) ν_{max} 3727, 3004, 2980, 2960, 2357, 2335, 2300, 1779, 1717, 1653, 1457, 1350, 1260, 1177, 1098, 996, 931, 885, 866 cm^{-1}; ^1H NMR (600 MHz) and ^{13}C NMR (151 MHz), see Table 2; HRESIMS *m*/*z* 389.1571 $[M + Na]^+$ (calcd for $C_{19}H_{26}O_7Na$, 389.1576).

*Oidiolactone I (**7**):* white solid; $[\alpha]^{23}_D$ −63 (*c* 0.2, CH_2Cl_2); UV (CH_2Cl_2) λ_{max} (log ε) 205 (2.51), 230 (2.57), 245 (2.58), 285 (2.55); IR (film) ν_{max} 3747, 3004, 2985, 2950, 2357, 2340, 2320, 1775, 1718, 1654, 1457, 1350, 1260, 1178, 1097, 1043, 995, 931, 885 cm^{-1}; ^1H NMR (600 MHz) and ^{13}C NMR (151 MHz), see Table 2; HRAPCI-MS *m*/*z* 321.1331 $[M + H]^+$ (calcd for $C_{17}H_{21}O_6$, 321.1338).

*Oidiolactone J (**12**):* white solid; $[\alpha]^{23}_D$ −112 (*c* 0.3, CH_2Cl_2); UV (CH_2Cl_2) λ_{max} (log ε) 205 (2.15), 230 (2.21), 245 (2.22), 295 (2.20); IR (film) ν_{max} 3740, 3005, 2985, 2357, 1755, 1703, 1455, 1275, 1261, 1200, 1115, 1051, 958 cm^{-1}; ^1H NMR (600 MHz) and ^{13}C NMR (151 MHz), see Table 3; HRAPCI-MS *m*/*z* 321.1328 $[M + H]^+$ (calcd for $C_{17}H_{21}O_6$, 321.1338).

*Oidiolactone K (**13**):* white solid ; $[\alpha]^{23}_D$ −180 (*c* 0.052, CH_2Cl_2); UV (CH_2Cl_2) λ_{max} (log ε) 205 (3.10), 230 (3.17), 245 (3.18); IR (film) ν_{max} 3707, 3005, 2989, 2359, 2340, 1790, 1705, 1699, 1575, 1560, 1508, 1456, 1275, 1260, 1202, 1100, 1054, 1032, 993, 922 cm^{-1}; ^1H NMR (600 MHz) and ^{13}C NMR (151 MHz), see Table 3; HRESIMS *m*/*z* 305.1049 $[M - H]^-$ (calcd for $C_{16}H_{17}O_6$, 305.1025).

https://dx.doi.org/10.1021/acs.jnatprod.9b00789
J. Nat. Prod. XXXX, XXX, XXX−XXX

*Oidiolactone L (**14**):* colorless needles; $[\alpha]^{23}_{D}$ +168 (*c* 0.025, CH_2Cl_2); UV (CH_2Cl_2) λ_{max} (log ε) 205 (2.47), 230 (2.54), 245 (2.54), 295 (2.52), 315 (2.52); IR (film) ν_{max} 3738, 3004, 2987, 2920, 2358, 2320, 2300, 1773, 1730, 1705, 1699, 1542, 1475, 1399, 1275, 1260, 1199, 1084, 995, 936 cm^{-1}; ^1H NMR (600 MHz) and ^{13}C NMR (151 MHz), see Table 3; HRAPCI-MS *m*/*z* 289.1088 $[M - H]^-$ (calcd for $C_{16}H_{17}O_5$, 289.1076).

*5-Chloroparietin (**17**):* orange solid; UV (MeOH/CH_2Cl_2, 1:1) λ_{max} (log ε) 205 (3.64), 230 (3.70), 245 (3.70), 295 (3.69), 435 (3.58); IR (film) ν_{max} 3766, 3001, 2991, 2922, 2851, 2359, 2341, 2328, 1717, 1637, 1540, 1457, 1357, 1336, 1274, 1260, 761, 751 cm^{-1}; ^1H NMR (DMSO-d_6, 400 MHz) 7.08 s (H-2), 7.35 s (H-4), 6.90 s (H-7), 2.39 s (CH_3-3), 3.88 s (OCH_3-6), and 13.1 s (OH-8); ^{13}C NMR (DMSO-d_6, 100 MHz) 160.8 (C-1), 123.0 (C-2), 146.4 (C-3), 118.7 (C-4), 133.5 (C-4a), 112.6 (C-5, interchangeable with C-8a), 160.8 (C-6), 104.6 (C-7), 161.4 (C-8), 114.7 (C-8a, interchangeable with C-5), 182.8 (C-9), 114.0 (C-9a), 182.8 (C-10), 132.6 (C-10a), 21.4 (CH_3-3), and 56.1 (OCH_3-6); HRAPCI-MS *m*/*z* 319.0398 $[M + H]^+$ (calcd for $C_{16}H_{12}ClO_5$, 319.0373).

Antimicrobial Bioassays. All compounds were tested against bacterial and yeast pathogens using a modified broth dilution assay (methicillin-resistant *Staphylococcus aureus* (MRSA) ATCC 43300, vancomycin-resistant *Enterococcus faecalis* (VRE) ATCC 51299, *Escherichia coli* ATCC 25922, *Acinetobacter baumannii* ATCC 19606, *Pseudomonas aeruginosa* ATCC 27853, *Klebsiella pneumonia* ATCC 13883, *Cryptococcus neoformans* ATCC 66031, and *Candida albicans* ATCC 10231).[44] The strains of *S. aureus*, *E. coli*, and *K. pneumoniae* were grown at 37 °C on Tryptic Soy media (TSA, TSB; BD Biosciences, San Jose, CA, USA). *A. baumannii* was routinely cultured at 37 °C on nutrient medium (BD Biosciences). Brain heart infusion (BHI; BD Biosciences) was used for the cultivation of VRE at 37 °C. Yeast malt (YM; BD Biosciences) media was used for cultivating *C. albicans* at 30 °C. *C. neoformans* was grown at 30 °C on Sabouraud dextrose (SD; BD Biosciences) media. Briefly, bacteria or yeasts were grown to mid log phase, diluted with fresh medium to an optical density at 600 nm (OD_{600}) of 0.030−0.060, and then diluted again 1:10. This suspension (195 μL) was added to wells in a 96-well microtiter plate (Sarstedt), and 5 μL of compound dissolved in DMSO was added to give a final concentration of 100−0.1 μM at 2.5% DMSO by volume. A DMSO negative control and standard antibiotic positive controls were included in each plate. All compounds were tested in triplicate for each concentration. Plates were sealed with Parafilm, placed in a Ziploc bag to prevent evaporation, and incubated at 30 °C (fungi) or 37 °C (bacteria) for 16−20 h (48 h for *C. neoformans*). The OD_{600} values for each well were determined with a plate reader (Biotek, EL800), and the data were standardized to the DMSO control wells after subtracting the background from the blank media wells. Select compounds and extracts were also tested against the fungal bat pathogen *Pseudogymnoascus destructans* (ATCC MYA 4855) using a similar broth dilution assay with the addition of 0.2% carageenan to SD media to facilitate dispersion of mycelia, a spore concentration of 2500 spores/mL, and incubation at 15 °C for ∼2 weeks.

Bat Fibroblast Tissue Culture. Wing tissue samples were obtained from bats captured by harp net at Sequiota Park in Springfield, MO (October 2017), and included gray bats (*Myotis grisescens*) and northern long-eared bats (*Myotis septentrionalis*). Permission for these collections was obtained from the Missouri Department of Conservation and United States Fish and Wildlife Service.

Upon capture, one biopsy was collected from each wing using a 3 mm biopsy punch. Punches from five bats per species (10 punches total) were pooled together to create enough tissue for further processing. Punches were briefly dipped in 70% ethanol and then transferred to a 1.5 mL microcentrifuge tube (pooled by species) containing 1.0 mL of Dulbecco's modified Eagle medium (DMEM). Samples were stored on ice for no more than 24 h for transport to Missouri State University.

To collect wing-derived fibroblasts, wing biopsies were stripped to the cellular level by incubating at 37 °C for 3 h in 1 mL of DMEM with collagenase type II. Fibroblasts were then manually isolated by pressing the tissue through a 70 μm cell strainer. Cells and collagenase medium were centrifuged for seven minutes at 400*g*. The medium was removed, and cells were plated with 50% fetal bovine serum (FBS)/50% DMEM. Antimicrobials were added to prevent growth of bacteria and fungus that may have been on the wings upon capture: ampicillin (100 μg/mL); penicillin and streptomycin (50 units/mL each); gentamycin (20 μg/mL); kanamycin (100 μg/mL); and aureobasidin A (0.5 μg/mL) or amphotericin B (2.5 μg/mL). Cells were allowed to grow at 37 °C in cell culture flasks, and medium was changed every 2 or 3 days for 2 weeks. At this point, the culture medium was switched to a standard medium with DMEM + 10% FBS + penicillin and streptomycin (50 units/mL each), and cells were cultured until confluent. Cells were then either used for experiments or stored for future use. Primary fibroblast cell cultures from both species were viable and consistent for approximately 20 passages.

To store fibroblasts for further experimentation, all growth media was removed, and the flask was incubated at 37 °C for 10 min with 2.5 mL of 0.25% Trypsin and 0.1% ethylenediaminetetraacetic acid in Hank's balanced salt solution to detach adherent cells. Then, 10 mL of DMEM was added to the flask and thoroughly mixed. Cells and medium were centrifuged for 7 min at 400*g*. The supernatant was discarded, and freezing media (90% FBS + 10% pure dimethyl sulfoxide, combined, and then 0.02 μm filtered) was mixed thoroughly with the cell pellet before being stored in 0.5−1 mL aliquots at −80 °C until needed.

Mammalian Fibroblast Cytotoxicity (MTT Cell Viability Assays).[45] *Myotis grisescens and M. septentrionalis* fibroblast cells were maintained in growth media: DMEM (Invitrogen 11965-092) supplemented with 10% FBS (Invitrogen 16000-044) and 1% penicillin/streptomycin (Invitrogen 15140-122). Human fibroblast cells were maintained in fibroblast basal growth media (ATCC# PCS-201-030) supplemented with a low-serum fibroblast growth kit (ATCC# PCS-201-041). Cells were plated in 96-well plates at ∼25 × 10^4 cells/mL and allowed to adhere overnight. After 24 h, compounds were added at nine concentrations, from 100 μM to 15.24 nM final concentration in growth media using 3-fold dilutions, in triplicate.

Plates were incubated for 72 h at 37 °C in humidified 5% CO_2/95% air, after which time the media was removed and 200 μL of thiazolyl blue tetrazolium bromide (1 mg/mL in water, Sigma M2128) was added in RPMI phenol red free media (Invitrogen 11835-030). The reagent was removed after 3 h, formazan crystals were solubilized with 200 μL of isopropanol, and plates were read on a Molecular Devices SpectraMax i3 plate reader at 570 nm for formazan and 690 nm for background subtraction. EC_{50} values and percent viability were calculated by fitting the data to a sigmoidal dose−response curve (variable slope) in GraphPad Prism software.

■ ASSOCIATED CONTENT

Supporting Information

The Supporting Information is available free of charge at https://pubs.acs.org/doi/10.1021/acs.jnatprod.9b00789.

Supplementary figures, NMR and mass data for new compounds, and CD spectra for select compounds (PDF)

Strain activity and taxonomy table (XLSX)

Oidiodendron isolates and activity table (XLSX)

■ AUTHOR INFORMATION

Corresponding Author

Christine E. Salomon − *Center for Drug Design, University of Minnesota, Minneapolis, Minnesota 55405, United States;* orcid.org/0000-0003-4976-598X; Phone: 612-626-3698; Email: csalomon@umn.edu; Fax: 612-625-8125

Authors

Yudi Rusman − *Center for Drug Design, University of Minnesota, Minneapolis, Minnesota 55405, United States*

Michael B. Wilson − *Center for Drug Design, University of Minnesota, Minneapolis, Minnesota 55405, United States*

Jessica M. Williams − *Center for Drug Design, University of Minnesota, Minneapolis, Minnesota 55405, United States*
Benjamin W. Held − *Department of Plant Pathology, University of Minnesota, Minneapolis, Minnesota 55405, United States*
Robert A. Blanchette − *Department of Plant Pathology, University of Minnesota, Minneapolis, Minnesota 55405, United States*
Brianna N. Anderson − *Department of Biology, Missouri State University, Springfield, Missouri 65897, United States*
Christopher R. Lupfer − *Department of Biology, Missouri State University, Springfield, Missouri 65897, United States*

Complete contact information is available at: https://pubs.acs.org/10.1021/acs.jnatprod.9b00789

Author Contributions

⊥Y. Rusman and M. B. Wilson contributed equally to this work.

Notes

The authors declare no competing financial interest.

■ ACKNOWLEDGMENTS

This work was funded by grant ML 2016 Chp 186, sec 2, from the Environmental and Natural Resources Trust Fund by the State of Minnesota to C.E.S. and R.A.B. and USFW F15AP01056 to C.E.S. and R.A.B. We thank J. Nugent for the human fibroblast cell line culture and G. Krause for assistance with the fungal assays. We are grateful to J. Essig, J. Pointer, and the Soudan Underground Mine State Park staff for facilitating field collections. We thank G. Nordquist for helpful discussions and field assistance and the Minnesota Department of Natural Resources for permits and logistical support.

■ REFERENCES

(1) Blehert, D. S.; Hicks, A. C.; Behr, M.; Meteyer, C. U.; Berlowski-Zier, B. M.; Buckles, E. L.; Coleman, J. T. H.; Darling, S. R.; Gargas, A.; Niver, R.; Okoniewski, J. C.; Rudd, R. J.; Stone, W. B. *Science* **2009**, *323*, 227.
(2) Lorch, J. M.; Meteyer, C. U.; Behr, M. J.; Boyles, J. G.; Cryan, P. M.; Hicks, A. C.; Ballmann, A. E.; Coleman, J. T. H.; Redell, D. N.; Reeder, D. M.; Blehert, D. S. *Nature* **2011**, *480*, 376−378.
(3) Minnis, A. M.; Lindner, D. L. *Fungal Biol.* **2013**, *117*, 638−649.
(4) Warnecke, L.; Turner, J. M.; Bollinger, T. K.; Lorch, J. M.; Misra, V.; Cryan, P. M.; Wibbelt, G.; Blehert, D. S.; Willis, C. K. R. *Proc. Natl. Acad. Sci. U. S. A.* **2012**, *109*, 6999−7003.
(5) Meteyer, C. U.; Buckles, E. L.; Blehert, D. S.; Hicks, A. C.; Green, D. E.; Shearn-Bochsler, V.; Thomas, N. J.; Gargas, A.; Behr, M. J. *J. Vet. Diagn. Invest.* **2009**, *21*, 411−414.
(6) Jachowski, D. S.; Dobony, C. A.; Coleman, L. S.; Ford, W. M.; Britzke, E. R.; Rodrigue, J. L. *Diversity and Distributions* **2014**, *20*, 1002−1015.
(7) Frick, W. F.; Puechmaille, S. J.; Hoyt, J. R.; Nickel, B. A.; Langwig, K. E.; Foster, J. T.; Barlow, K. E.; Bartonička, T.; Feller, D.; Haarsma, A.-J.; Herzog, C.; Horacek, I.; van der Kooij, J.; Mulkens, B.; Petrov, B.; Reynolds, R.; Rodrigues, L.; Stihler, C. W.; Turner, G. G.; Kilpatrick, A. M. *Glob. Ecol. Biogeogr.* **2015**, *24*, 741−749.
(8) Boyles, J. G.; Cryan, P. M.; McCracken, G. F.; Kunz, T. H. *Science* **2011**, *332*, 41−42.
(9) Rocke, T. E.; Kingstad-Bakke, B.; Wüthrich, M.; Stading, B.; Abbott, R. C.; Isidoro-Ayza, M.; Dobson, H. E.; Dos Santos Dias, L.; Galles, K.; Lankton, J. S.; Falendysz, E. A.; Lorch, J. M.; Fites, J. S.; Lopera-Madrid, J.; White, J. P.; Klein, B.; Osorio, J. E. *Sci. Rep.* **2019**, *9*, 6788.
(10) Palmer, J. M.; Drees, K. P.; Foster, J. T.; Lindner, D. L. *Nat. Commun.* **2018**, *9*, 35.
(11) Chaturvedi, S.; Rajkumar, S. S.; Li, X.; Hurteau, G. J.; Shtutman, M.; Chaturvedi, V. *PLoS One* **2011**, *6*, e17032.
(12) Kulhanek, T. C. *The Application of Chitosan on an Experimental Infection of Pseudogymnoascus Destructans Increases Survival in Little Brown Bats*; Western Michigan University, 2016.
(13) Frank, C. L.; Ingala, M. R.; Ravenelle, R. E.; Dougherty-Howard, K.; Wicks, S. O.; Herzog, C.; Rudd, R. J. *PLoS One* **2016**, *11*, e0153535.
(14) Padhi, S.; Dias, I.; Korn, V. L.; Bennett, J. W. *J. Fungi (Basel)* **2018**, *4*, DOI: 10.3390/jof4020048.
(15) Cornelison, C. T.; Gabriel, K. T.; Barlament, C.; Crow, S. A., Jr. *Mycopathologia* **2014**, *177*, 1−10.
(16) Cornelison, C. T.; Keel, M. K.; Gabriel, K. T.; Barlament, C. K.; Tucker, T. A.; Pierce, G. E.; Crow, S. A. *BMC Microbiol.* **2014**, *14*, 246.
(17) Lorch, J. M.; Muller, L. K.; Russell, R. E.; O'Connor, M.; Lindner, D. L.; Blehert, D. S. *Appl. Environ. Microbiol.* **2013**, *79*, 1293−1301.
(18) Micalizzi, E. W.; Mack, J. N.; White, G. P.; Avis, T. J.; Smith, M. L. *PLoS One* **2017**, *12*, e0179770.
(19) Hoyt, J. R.; Cheng, T. L.; Langwig, K. E.; Hee, M. M.; Frick, W. F.; Kilpatrick, A. M. *PLoS One* **2015**, *10*, e0121329.
(20) Cheng, T. L.; Mayberry, H.; McGuire, L. P.; Hoyt, J. R.; Langwig, K. E.; Nguyen, H.; Parise, K. L.; Foster, J. T.; Willis, C. K. R.; Kilpatrick, A. M.; Frick, W. F. *J. Appl. Ecol.* **2017**, *54*, 701−708.
(21) Wilson, M. B.; Held, B. W.; Freiborg, A. H.; Blanchette, R. A.; Salomon, C. E. *PLoS One* **2017**, *12*, e0178968.
(22) Badalamenti, J. P.; Erickson, J. D.; Salomon, C. E. *Genome Announc.* **2016**, *4*, e00290−16.
(23) Rusman, Y.; Held, B. W.; Blanchette, R. A.; Wittlin, S.; Salomon, C. E. *J. Nat. Prod.* **2015**, *78*, 1456−1460.
(24) Hosoe, T.; Nozawa, K.; Lumley, T. C.; Currah, R. S.; Fukushima, K.; Takizawa, K.; Miyaji, M.; Kawai, K. *Chem. Pharm. Bull.* **1999**, *47*, 1591−1597.
(25) John, M.; Krohn, K.; Flörke, U.; Aust, H. J. *J. Nat. Prod.* **1999**, *62*, 1218−1221.
(26) Andersen, N. R.; Rasmussen, P. R. *Tetrahedron Lett.* **1984**, *25*, 465−468.
(27) Ellestad, G. A.; Evans, R. H.; Kunstmann, M. P. *Tetrahedron Lett.* **1971**, *12*, 497−500.
(28) Ellestad, G. A.; Evans, R. H.; Kunstmann, M. P. *J. Am. Chem. Soc.* **1969**, *91*, 2134−2136.
(29) Ellestad, G. A.; Evans, R. H.; Kunstmann, M. P.; Lancaster, J. E.; Morton, G. O. *J. Am. Chem. Soc.* **1970**, *92*, 5483−5489.
(30) Danielsen, K.; Aksnes, D. W.; Francis, G. W. *Magn. Reson. Chem.* **1992**, *30*, 359−360.
(31) Stevanović, D.; Damljanović, I.; Vukićević, M.; Manojlović, N.; Radulović, N. S.; Vukićević, R. D. *Health Care Anal.* **2011**, *94*, 1406−1415.
(32) Sargent, M. V.; Smith, D. O.; Elix, J. A. *J. Chem. Soc. C* **1970**, *2*, 307−311.
(33) Barrero, A. F.; Sánchez, J. F.; Elmerabet, J. *Tetrahedron Lett.* **1995**, *36*, 5251−5254.
(34) Lee, J. K.; Kim, D. B.; Kim, J. I.; Kim, P. Y. *Toxicol. In Vitro* **2000**, *14*, 345−349.
(35) Reynolds, H. T.; Ingersoll, T.; Barton, H. A. *J. Wildl. Dis.* **2015**, *51*, 318−331.
(36) Lorch, J. M.; Lindner, D. L.; Gargas, A.; Muller, L. K.; Minnis, A. M.; Blehert, D. S. *Mycologia* **2013**, *105*, 237−252.
(37) Man, B.; Wang, H.; Xiang, X.; Wang, R.; Yun, Y.; Gong, L. *Front. Microbiol.* **2015**. *6*, DOI: 10.3389/fmicb.2015.01158.
(38) Rice, A. V.; Currah, R. S. *Stud. Mycol.* **2005**, *53*, 83−120.
(39) Zhang, T.; Victor, T. R.; Rajkumar, S. S.; Li, X.; Okoniewski, J. C.; Hicks, A. C.; Davis, A. D.; Broussard, K.; LaDeau, S. L.; Chaturvedi, S.; Chaturvedi, V. *PLoS One* **2014**, *9*, e108714.
(40) Couture, M.; Fortin, J. A.; Dalpe, Y. *New Phytol.* **1983**, *95*, 375−380.
(41) Kernaghan, G.; Patriquin, G. *Microb. Ecol.* **2011**, *62*, 460−473.
(42) Kearse, M.; Moir, R.; Wilson, A.; Stones-Havas, S.; Cheung, M.; Sturrock, S.; Buxton, S.; Cooper, A.; Markowitz, S.; Duran, C.; Thierer, T.; Ashton, B.; Meintjes, P.; Drummond, A. *Bioinformatics* **2012**, *28*, 1647−1649.

(43) Lane, D. J. In *Nucleic Acid Techniques in Bacterial Systematics*; Stackebrandt, E.; Goodfellow, M., Eds.; Wiley: New York, 1991; pp 115−175.
(44) *Performance Standards for Antimicrobial Susceptibility Testing: 14th Informational Supplement*; National Committee for Clinical Laboratory Standards: Wayne, PA, 2004.
(45) Mosmann, T. *J. Immunol. Methods* **1983**, *65*, 55−63.

https://dx.doi.org/10.1021/acs.jnatprod.9b00789
J. Nat. Prod. XXXX, XXX, XXX−XXX